PRAMANA
— journal of
physics

Vol. 57, Nos 2 & 3
Aug. & Sept. 2001
pp. 271–283

Searching for quark matter with dileptons and photons: From SPS to relativistic heavy-ion collider

ITZHAK TSERRUYA
Weizmann Institute of Science, Rehovot 76100, Israel
Email: Itzhak.Tserruya@weizmann.ac.il.

Abstract. The heavy-ion programme at the CERN SPS, which started back in '86, has produced a wealth of very interesting and intriguing results in the quest for the quark-gluon plasma. The highlights of the programme on dilepton and direct photon measurements are reviewed emphasizing the most recent results obtained in Pb–Pb collisions at 158 A GeV. Prospects from RHIC are discussed.

Keywords. Quark-gluon plasma; chiral symmetry restoration; relativistic heavy-ion collisions; dileptons; photons.

PACS No. 25.75.-q

1. Introduction

The heavy-ion programme at the CERN SPS started in 1986 with the acceleration of O beams at an energy of 200 GeV/c per nucleon, later followed by a S beam at the same energy. Since 1994 the experiments used a Pb beam at a maximum energy of 158 GeV/c per nucleon ($\sqrt{s_{NN}} = 17.2$ GeV/c). The primary scientific objective is the search for the predicted phase transition associated with quark-gluon plasma formation and chiral symmetry restoration, using relativistic nuclear collisions to achieve in the laboratory the necessary conditions of temperature and density.

The CERN programme has produced a wealth of very interesting and intriguing results in the quest for the quark-gluon plasma. From systematic studies of global observables, particle distributions, production rates and correlations, a picture of a chemically and thermally equilibrated system undergoing collective expansion has emerged. The observation of J/ψ suppression, strangeness enhancement and excess emission of low-mass lepton pairs are among the most notable results hinting at new physics [1].

The relativistic heavy-ion collider (RHIC) at BNL started regular operations in the summer of 2000, opening a new era in the study of ultrarelativistic heavy-ion collisions, at energies up to $\sqrt{s_{NN}} = 200$ GeV/c, more than one order of magnitude larger than at CERN. The higher c.m. energies result in much better conditions (higher energy density, higher temperature, longer lifetime) for the study of quark matter.

The advent of RHIC seems to be an appropriate time to summarize the achievements at CERN and to put them in perspective with respect to the expectations from RHIC. The

discussion in this paper is restricted to electromagnetic probes, dilepton and photon measurements, only.

The interest in dileptons and photons stems from their relatively large mean free path. As a consequence, they can leave the interaction region without final state interaction, carrying information about the conditions and properties of the matter at the time of their production and in particular of the early stages of the collision when temperature and energy density have their largest values, i.e. when the conjectured deconfinement and chiral symmetry restoration phase transition is expected to take place. This has to be contrasted with the hadronic observables which are sensitive to the late stages at, or after freeze-out, when the hadronic system stops interacting.

A prominent topic of interest is the identification of thermal radiation emitted from the collision system. This radiation should tell us the nature of the matter formed, a quark-gluon plasma (QGP) or a high-density hadron gas (HG).

The physics potential of dileptons is further emphasized by the capability to measure the vector mesons ρ, ω and ϕ, through their leptonic decays. Of particular interest is the ρ meson since it provides a unique opportunity to observe in-medium modifications of the vector meson properties (mass and/or width) which might be linked to chiral symmetry restoration. Due to its very short lifetime ($\tau = 1.3$ fm/c) compared to the typical fireball lifetime of ~ 10 fm/c at SPS energies, most of the ρ mesons decay inside the interaction region with eventually modified properties. The situation is different for the ω and ϕ mesons. Because of their much longer lifetimes they predominantly decay outside the interaction region after having regained their vacuum properties.

The CERN experiments have confirmed the unique physics potential of these electromagnetic probes. A compilation of all measurements performed so far is presented in table 1 together with the kinematic phase space covered and relevant references. The programme involved systematic studies with p, S and Pb beams and the most notable results will be reviewed below.

2. Low-mass dileptons

2.1 *Experimental results*

The low-mass region, m = 200–600 MeV/c^2, has been systematically studied by the CERES experiment including measurements of p–Be (a very good approximation to pp collisions) and p–Au at 450 GeV/c [2,3], S–Au at 200 GeV per nucleon [4], and Pb–Au at 158 GeV per nucleon [5–7] and 40 GeV per nucleon [8]. The Pb–Au results at 158 GeV per nucleon were obtained in two different runs, in 1995 [5,6] and 1996 [7]. Apart from a slight difference in the centrality trigger ($\langle \mathrm{d}n_{\mathrm{ch}}/\mathrm{d}\eta \rangle = 250$ and 220 in the '96 and '95 runs, respectively), the two measurements were performed under identical conditions and yielded consistent results within their systematic uncertainties. Figure 1 shows the dilepton invariant mass spectrum of the '96 Pb–Au run at 158 GeV per nucleon as well as the preliminary results obtained in the '99 Pb–Au run at 40 GeV per nucleon. In both cases the dilepton yield is normalized to the measured charged particle yield within the CERES acceptance ($2.1 < \eta < 2.65$).

The solid lines represent the expected yield from known hadronic sources based on a generator [7] which uses measured particle production ratios whenever available or ratios

Table 1. List of measurements at the CERN SPS.

Dileptons					
Experiment	Probe	System	y	Mass (GeV/c^2)	Ref.
CERES	e^+e^-	p–Be, Au 450 GeV/c S–Au 200 GeV/u Pb–Au 158 GeV/u 40 GeV/u	2.1–2.65	0 – 1.4	[2,3] [4] [5–7] [8]
HELIOS-1	$\mu^+\mu^-$	p–Be 450 GeV/c	3.65–4.9	0.3 – 4.0	[9]
(completed)	e^+e^-	p–Be 450 GeV/c	3.15–4.65	0.3 – 4.0	[9]
HELIOS-3 (completed)	$\mu^+\mu^-$	p–W, S-W 200 GeV/u	> 3.5	0.3 – 4.0	[10]
NA38	$\mu^+\mu^-$	p–A, S–U 200 GeV/u	3.0–4.0	0.3 – 6.0	[11]
NA50	$\mu^+\mu^-$	Pb–Pb 158 GeV/u	3.0–4.0	0.3 – 7.0	[12]

Photons				
Experiment	System	y	p_t (GeV/c)	Ref.
CERES	S–Au 200 GeV/u	2.1–2.7	0.4–2.0	[13]
	Pb–Au 158 GeV/u	2.1–2.7	0.4–2.0	
HELIOS-2 (completed)	p, O, S–W 200 GeV/u	1.0–1.9	0.1–1.5	[14]
WA80/ WA98	O–Au 200GeV/u	1.5–2.1	0.4–2.8	[15]
(completed)	S–Au 200 GeV/u	2.1–2.9	0.5–2.5	[16]
	Pb–Au 158 GeV/c	2.1–2.9	0.5–2.5	[17]

calculated with a thermal model which describes well all measured ratios [18,18b]. As previously observed with the S beam [4], the low-mass continuum in Pb–Au collisions is strongly enhanced with respect to this cocktail, both at 158 GeV per nucleon and at the much lower energy of 40 GeV per nucleon. For example, in the mass region $m = 0.25$–0.7 GeV/c^2, the enhancement factor (defined as the ratio of the measured to the calculated yield) at 158 GeV per nucleon is 2.6 ± 0.5 (stat.) $\pm$ 0.6 (syst.).

CERES has further characterized the properties of the low-mass excess. The results indicate that it is mainly due to pairs with soft p_t and that it increases faster than linearly with the event multiplicity [5–7]. The latter point is illustrated in figure 2 which displays the enhancement factor as function of the charged particle rapidity density for four mass intervals. Since the calculated yield increases linearly with multiplicity, a constant enhancement factor indicates that the data also increases linearly with multiplicity, as is the case for the very low-masses, in the region of the π^0 Dalitz decay. However, in the mass interval $0.25 < m < 0.68$ GeV/c^2 the measured yield increases stronger than linearly.

An enhancement of low-mass dileptons has also been observed in the di-muon experiments [10–12]. Whereas the $p-U$ data of NA38 are well reproduced by a cocktail of

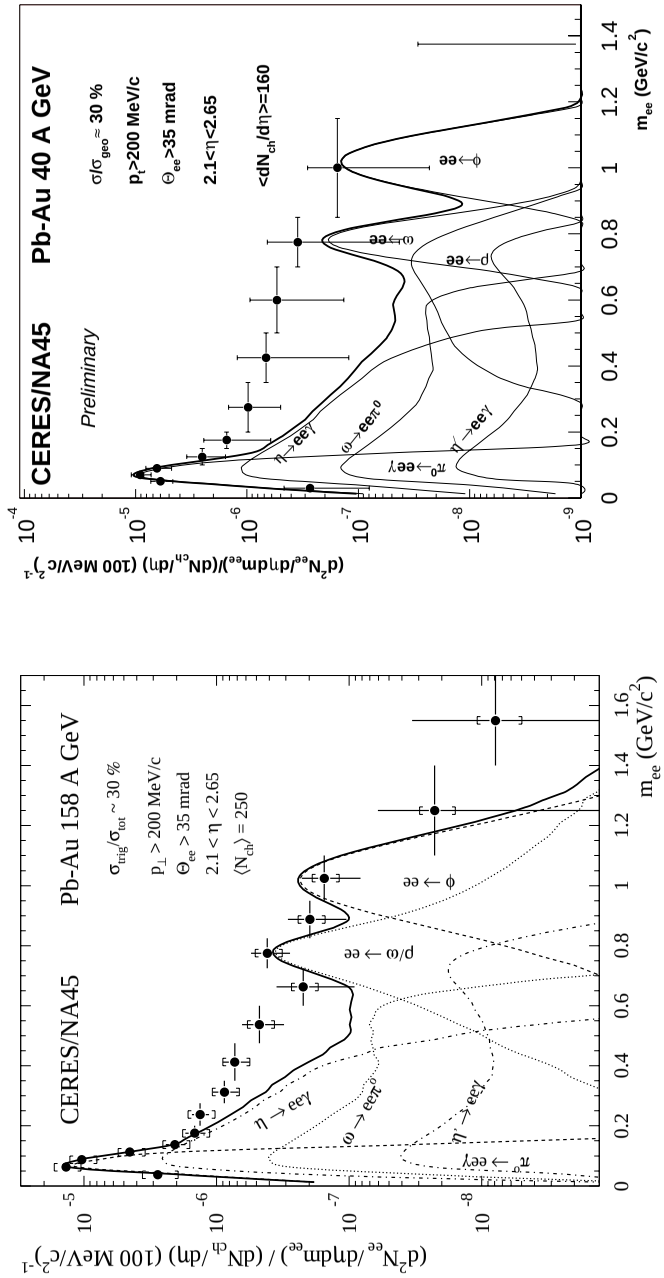

Figure 1. Inclusive e^+e^- mass spectrum measured by CERES in 158 A GeV Pb–Au collisions in the '96 run (left panel) [7] and 40 A GeV (right panel) [8]. The figures also show the summed (thick solid line) and individual (dotted lines in the left panel and thin lines in the right panel) contributions from hadronic sources.

hadronic sources (with the somewhat uncertain extrapolation of the Drell–Yan contribution into low masses), the S data show an enhancement of low-mass pairs which is hardly noticeable in the Pb–Pb collisions (see figure 3). In both cases the enhancement is clearly visible in the ϕ meson and extends over the intermediate mass region.

There is a striking difference in the shape of the low-mass dilepton spectrum as measured by CERES and NA38/50. The latter exhibits a pronounced structure due to the resonance decays whereas in the CERES results the structure is completely washed out (see figure 1). Resolution effects are certainly not responsible for this difference since the low-mass spectrum in p–Be and p–Au collisions measured by CERES with the same apparatus clearly shows the ρ/ω peak [2]. We also note that the two experiments cover nearly symmetric ranges around mid-rapidity ($\eta = 2.1-2.65$ and $\eta = 3-4$ in CERES and NA38, respectively). But CERES has a relatively low p_t cut of 200 MeV/c on each track whereas NA38 is restricted to $m_t > 0.9 + 2(y_{\rm lab} - 3.55)^2$ GeV/c^2. NA50 has an even stronger m_t cut, $m_t > 1.3 + 2(y_{\rm lab} - 3.55)^2$ GeV/c^2. Moreover, NA38/50 have no centrality selection in the trigger whereas the CERES data corresponds to the top 30% of the geometrical cross section. These two factors are likely to explain the apparent discrepancy since, as noted previously, the excess observed by CERES is more pronounced at low pair p_t and increases stronger than linearly with multiplicity. Given enough statistics it should be fairly easy for the two experiments to apply common m_t and centrality cuts thereby allowing a direct and meaningful comparison between their results. Such a comparison should be possible once results from the newly approved experiment NA60 at CERN become available [19].

2.2 *Theoretical evaluation*

The enhancement of low-mass dileptons has triggered a wealth of theoretical activity. Dozens of articles have been published on the subject and only a summary of the most prominent approaches and current open issues is presented here. (For a comprehensive review see [20]).

There is consensus that a simple superposition of pp collisions cannot explain the data and that an additional source is needed. The pion annihilation channel ($\pi^+\pi^- \rightarrow \rho \rightarrow l^+l^-$), obviously not present in pp collisions, has to be added to the cocktail. This channel provides first evidence of thermal radiation from a dense hadron gas and accounts for a large fraction of the observed enhancement. However, it is not sufficient to reproduce the data in the mass region $0.2 < m_{e^+e^-} < 0.6$ GeV/c^2. These data have been quantitatively explained by taking into account in-medium modifications of the vector mesons. Li, Ko and Brown [21] were the first to propose a decrease of the ρ-meson mass in the hot and dense fireball as a precursor of chiral symmetry restoration, following the original Brown–Rho scaling [22]. With this approach, an excellent agreement with the CERES data is achieved as demonstrated by the solid line (taken from [23]) in figure 4. Another avenue, based on effective Lagrangians, uses a ρ-meson spectral function which takes into account the ρ propagation in hot and dense matter, including in particular the pion modification in the nuclear medium and the scattering of ρ mesons off baryons [24]. This leads to a large broadening of the ρ-meson line shape and consequently to a considerable enhancement of low-mass dileptons. These calculations also achieve an excellent reproduction of the CERES results as illustrated by the dashed line in figure 4. Although the two approaches are different in the underlying physical picture (in the Brown–Rho scaling the constituent

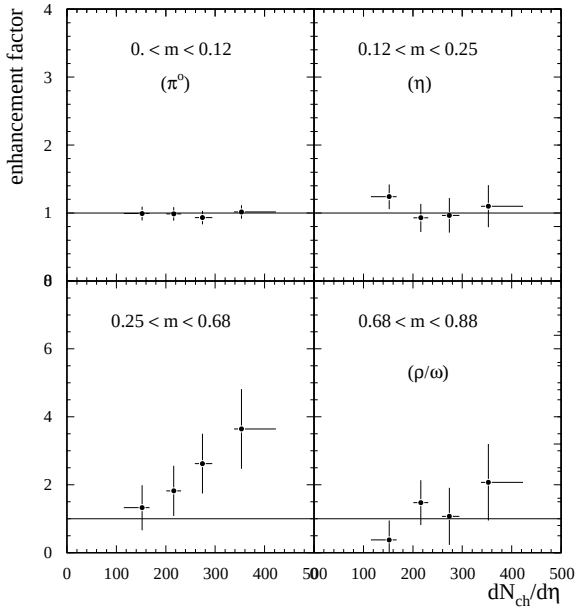

Figure 2. Multiplicity dependence of the enhancement factor for four mass intervals obtained by CERES in Pb–Au collisions at 158 GeV per nucleon in the '96 run [7].

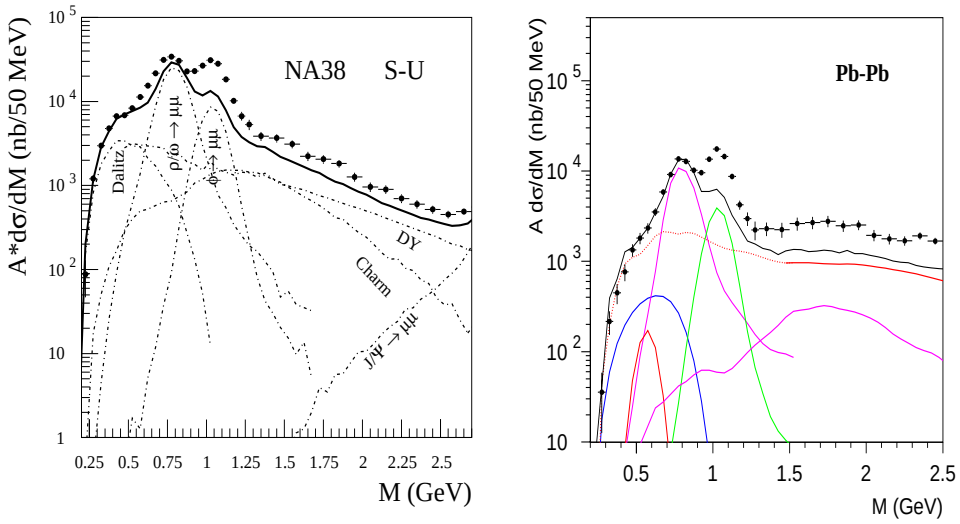

Figure 3. Inclusive $\mu^+\mu^-$ mass spectra measured by NA38 in 200 A GeV S–U collisions (left panel) [11] and by NA50 in 158 A GeV Pb–Pb collisions (right panel) [12]. The summed yield of all known sources is shown as well as the individual contributions.

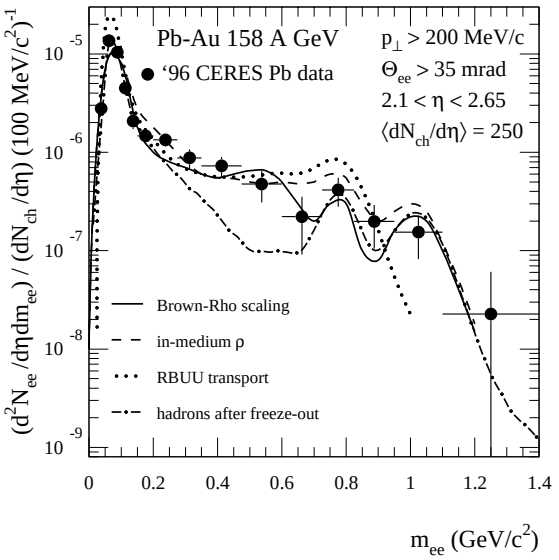

Figure 4. CERES results compared to calculations using dropping ρ mass (Brown–Rho scaling), in-medium ρ-meson broadening and RBUU transport model. The dash-dotted line represents the yield from hadrons after freeze-out as in figure 1.

quarks are the relevant degrees of freedom whereas ref. [24] relies on a hadronic description), it turns out that the dilepton production rates calculated via hadronic and partonic models are very similar at SPS conditions, down to masses of about 0.5 GeV/c^2 [20,23]. This 'quark-hadron duality' explains the similar results obtained with the two approaches.

Several issues still remain controversial. First, the Brown–Rho scaling hypothesis is not free of debate. Second, both models, the dropping mass and the collision broadening of the ρ meson, rely on a high baryon density. However, the role of baryons is still an open question. Calculations based on chiral reduction formulae, although similar in principle to those of [24], find very little effect due to baryons and are in fact low compared to the data [25]. The RBUU transport calculations of Koch [26] find also very little effect due to the baryons and come to a reasonably close description of the data as shown in figure 4 by the dotted line. However, the agreement is achieved by overestimating the ω yield (and the ω Dalitz decay yield) as clearly seen in the figure in the mass region $m \sim 800$ MeV, which is dominated by the $\omega \to e^+e^-$ decay. The CERES dilepton results in Pb–Au collisions at 40 GeV per nucleon (see figure 1 right panel) could be very valuable in this debate. One of the incentives for this measurement was indeed to study the effect of varying the baryon density which is expected to reach a maximum value, at least a factor of two larger than at 158 GeV per nucleon [27], at this low energy. Finally, there is a discrepancy between transport [28] and hydrodynamic calculations [29] in treating the time evolution of the fireball, the former yielding a factor of 2–3 higher yields.

In a recent paper, Schneider and Weise argue that the CERES enhancement can be entirely explained by thermal radiation emitted by the quark-gluon plasma through $\bar{q}q$ annihilation [30]. This is an interesting claim but also a surprising one since several previous

studies came to the conclusion that the plasma phase shines too little with respect to the hadronic sources [31].

3. Intermediate mass dileptons

An excess of dileptons has also been observed in the intermediate mass region $1.5 < m < 3.0$ GeV/c^2 by HELIOS-3 [10] and NA38/50 [11,12] (see figure 3). The excess refers to the expected yield from Drell–Yan and semi-leptonic charm decay which are the two main contributions in this mass region. The shape of the excess is very similar to the open charm contribution and in fact doubling the latter nicely accounts for the excess. This is the basis for the hypothesis of enhanced charm production put forward by NA38/50 [12]. However it seems unlikely that at SPS energies charm production could be enhanced by such a large factor [32]. HELIOS-3 points into a different direction. The excess plotted as a function of the dimuon transverse mass can be fitted by a single exponential shape below and above the resonance decays [10], suggesting a common origin of the excess in the low and intermediate mass regions. Following this line, Li and Gale [33] calculated the invariant dimuon spectrum in central S–W collisions at 200 A GeV. On top of the *physics* background of Drell–Yan and open charm pairs, they considered the thermal radiation of muon pairs resulting from secondary meson interactions including higher resonances and in particular the $\pi a_1 \rightarrow l^+l^-$. The calculations are based on the same relativistic fireball model that successfully reproduces the low-mass dileptons discussed in the previous section [21]. Whereas they could reproduce the low-mass data only with the dropping mass scenario, in the intermediate mass region the difference between free and in-medium meson masses with respect to the data is not so large. The calculations with free masses slightly overestimate the data whereas with dropping masses the situation is reversed. The intermediate mass region alone cannot therefore be used to support the dropping mass model, however it is important that the model can simultaneously explain the low and intermediate mass regions.

Recent calculations [34,35] were also able to explain the NA50 enhancement in the intermediate mass region as originating from thermal radiation. Rapp and Shuryak [34] exploit the quark-hadron duality and use the $q\overline{q}$ annihilation rates to calculate the dilepton yield throughout the entire space-time evolution of the collision which they describe with a simple fireball model. The thermal radiation, added to the 'background' (Drell–Yan and open charm) contributions, reproduces the NA50 enhancement observed in the mass range $1.5 < m < 3.0$ GeV/c^2 as shown in figure 5 (left panel). Only a small fraction of this radiation is emitted at the early stages and is associated with the QGP phase. Their calculations also reproduce the transverse momentum dependence of the muon pairs in the same mass interval (see figure 5 right panel).

4. Direct photons

Direct photons are expected to provide analogous information to thermal dileptons since real and virtual photons should carry the same physics information. However, the physics background for real photons (mainly from π^0 and η decays) is larger by orders of magnitude compared to dileptons (at $m > 200$ MeV/c^2), making the measurement of photons much less sensitive to a new source. And indeed, in contrast with the dilepton results, there is no clear evidence of enhancement in the measurements of real photons. All experiments

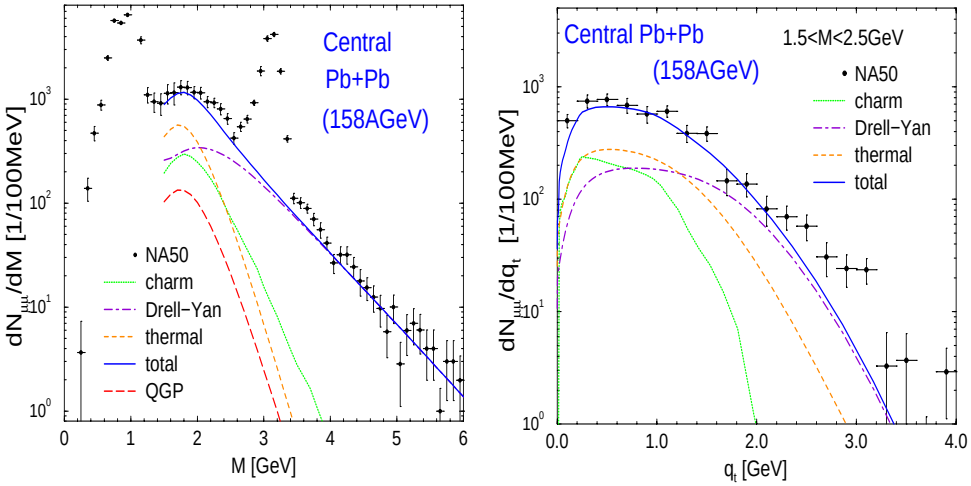

Figure 5. NA50 dimuon data (left panel: invariant mass spectrum, right panel: transverse momentum spectrum) compared to calculations of Rapp and Shuryak [34]. The various contributions (open charm, Drell–Yan, thermal radiation) and their sum are indicated in the figures.

performed with O and S beams have been able to establish only an upper limit for the production of thermal photons, which is of the order of 10–15% of the expected yield from hadron decays. The sensitivity is actually limited not by statistics but by the systematic errors. The S–Au results have been quantitatively reproduced [36] by the same fireball model, including dropping masses, used to explain the CERES and HELIOS-3 dilepton results. The calculations predict an excess of direct photons with respect to the hadronic background of a few percent, in agreement with the experimental results and with a simple estimate based on order of magnitude considerations [37]. In Pb–Pb collisions at 158A GeV a somewhat larger effect has been reported by WA98 [17]. In central collisions, a direct photon yield of $\sim 20\%$ is observed at $p_t > 1.5$ GeV/c whereas for peripheral collisions no excess is observed, as illustrated in figure 6 where the ratio of the measured photons to the calculated photons from hadronic sources is plotted as a function of p_t. Given the errors as indicated in the figure, the direct photon yield is only 1σ effect.

The p_t spectrum of the direct photons, defined as the difference between the measured photon and the hadronic background, is shown in figure 7. The data of S–Au collisions scaled by a factor of 3.5 [38] are also included. The error bars represent statistical and systematic errors added in quadrature. Data points with downward errors represent the 90%CL upper limit of the direct yield. The figure also displays results of calculations assuming the initial formation of a quark-gluon plasma, which expands, cools down, hadronizes and finally freezes out [38]. The calculations describe the data very well with the sum of almost equal contributions from prompt and thermal photons. The latter includes photons from the deconfined phase (calculated with the corrected two-loop rates [39]) and the hadron phase. At low p_t the quark matter contribution is relatively small whereas at high p_t it appears to be the dominant source of thermal radiation.

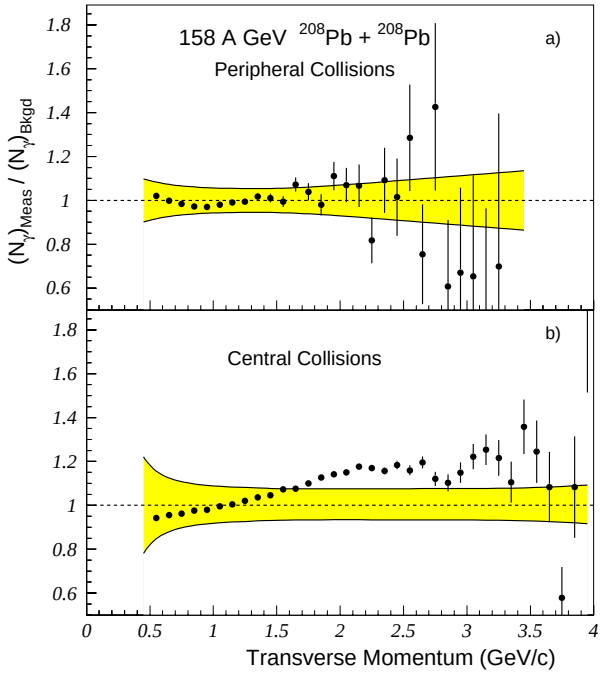

Figure 6. WA98 photon data in Pb–Pb peripheral (top panel) and central (lower panel) collisions at 158 A GeV. The error bars represent the statistical errors whereas the shaded bands indicate the systematic errors [17].

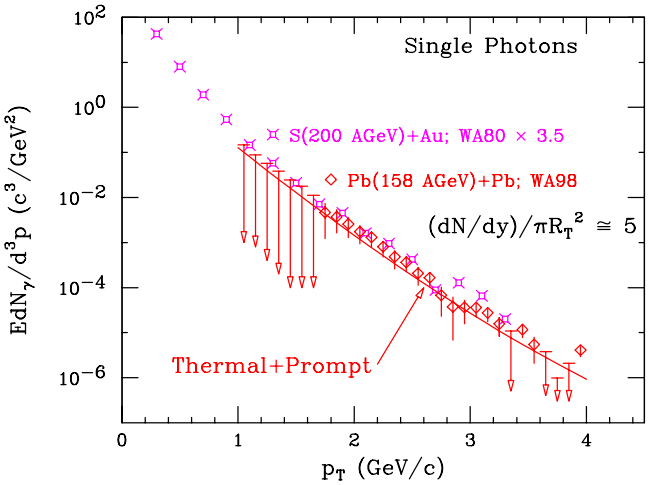

Figure 7. Single photon data in S–Au collisions from WA80 experiment scaled by a factor of 3.5 and in Pb–Pb central collisions from WA98 experiment compared to calculations from ref. [38].

Table 2. Conditions at RHIC year-1 running relative to SPS.

	RHIC Au + Au	SPS Pb + Pb
$\sqrt{s_{NN}}$ (GeV)	130	17.2
$\mathrm{d}N_{\mathrm{ch}}/\mathrm{d}y\ \ (y=0)^{(\mathrm{a})}$	750	410
$\mathrm{d}E_t/\mathrm{d}y\ \ (y=0)$ [GeV]	$688^{(\mathrm{b})}$	$405^{(\mathrm{c})}$
ϵ [GeV/fm^3]$^{(\mathrm{b})}$	5.0	2.9
$\bar{p}/p\ \ (y=0)$	$0.60^{(\mathrm{d})}$	$0.07^{(\mathrm{e})}$

$^{(\mathrm{a})}$See ref. [41] for details of the quoted values; $^{(\mathrm{b})}$see ref. [42] for details of the quoted values; $^{(\mathrm{c})}$see ref. [43]; $^{(\mathrm{d})}$see refs. [44]; $^{(\mathrm{e})}$see ref. [45].

5. RHIC opportunities

RHIC will allow the study of Au–Au collisions up to a maximum energy of $\sqrt{s_{NN}} = 200$ GeV. This unprecedented energy, more than one order of magnitude higher than at the SPS, will offer the possibility to extend the studies of quark matter under much better conditions. The higher collision energies will result in higher initial temperatures or equivalently in higher initial energy densities. This will lead to longer lifetimes and larger volumes allowing for a better study of the system before it freezes out and in particular of the early stages. In addition, the ability of RHIC to produce beams of different energies and species guarantees a systematic and comprehensive study of nuclear collisions from the elementary pp collisions to p-nucleus, and from light nuclei up to Au–Au collisions.

The first RHIC run on Au–Au collisions at $\sqrt{s_{NN}} = 130$ GeV took place in the summer of year 2000. From a short and relatively very low luminosity run, the four experiments were able to obtain an impressive amount of results, mainly in the hadronic sector, covering global observables, negative, positive and identified particle spectra, particle ratios, two particle correlations, flow studies and more. The results were presented at the Quark Matter Conference which took place at Stony Brook a few months after the RHIC year-1 data taking [40] and they allow to make a quantitative comparison of the main characteristics of central nuclear collisions at RHIC relative to the SPS. Some of them are listed in table 2. Both the charged particle rapidity density and the transverse energy are $\sim 70-80\%$ larger at RHIC than at SPS. Using the Bjorken prescription [46], this translates into at least a similar increase of the energy density depending on how much shorter the formation time at RHIC is compared to the SPS.

The low luminosity of RHIC year-1 run is clearly insufficient to address any of the physics topics discussed in this paper. However, from the unique features of RHIC one can expect drastic differences. As discussed above, the CERN results provide evidence of thermal radiation from a dense hadron gas whereas no clearly convincing evidence was found of electromagnetic radiation directly emitted from the QGP. The improved conditions at RHIC should facilitate the direct observation of this radiation thus providing a key element in the quest for quark-gluon plasma formation in nuclear collisions. The radiation

should be observable in principle in the direct photon channel and in the dilepton channel. At initial temperatures likely to be reached at RHIC, theory has singled out the dilepton mass range of 1–3 GeV/c^2 as the most suitable window to observe the thermal radiation from the QGP phase [47,48].

Another interesting difference might be in the role of baryons. Theory explains the low-mass pair enhancement observed at CERN by invoking in-medium modifications of the ρ meson properties as precursor of chiral symmetry restoration and, as discussed in §2.2, baryon density is the major factor responsible for these modifications both in the dropping mass and in the collision broadening scenarios. At RHIC, conditions of higher charged particle densities and hence higher temperatures may offer the possibility to explore a new domain where temperature rather than baryon density would be the dominant factor. The first RHIC results show that the net-baryon density is indeed much smaller than at the SPS, although it is clearly not yet net-baryon free. As shown in table 2, the $\bar{p}/p$ ratio increases from $\sim$0.07 at the SPS [45] to 0.60–0.65 at RHIC [44,49]. However, the relevant factor is not the net baryon but the total baryon density and if there is substantial baryon/antibaryon production at RHIC (no absolute values have been reported yet) the role of baryons could still be a significant one.

Among the four different experiments at RHIC, the PHENIX experiment is particularly focussed on the measurement of electromagnetic probes and is expected to address all these issues. First results should become available with the expected higher luminosity of RHIC year-2 running.

Acknowledgement

This work was supported by the Israeli Science Foundation, the MINERVA Foundation and the US-Israel Binational Science Foundation.

References

[1] See e.g. the Proceedings of Quark Matter 99 published in *Nucl. Phys.* **A661**
[2] CERES Collaboration: G Agakichiev *et al*, *Europhys. J.* **C4**, 231 (1998)
[3] CERES Collaboration: G Agakichiev *et al*, *Europhys. J.* **C4**, 249 (1998)
[4] CERES Collaboration: G Agakichiev *et al*, *Phys. Rev. Lett.* **75**, 1272 (1995)
[5] CERES Collaboration: I Ravinovich, *Nucl. Phys.* **A638**, 159c (1998)
[6] CERES Collaboration: G Agakichiev *et al*, *Phys. Lett.* **B422**, 405 (1998)
[7] CERES Collaboration: B Lenkeit, *Nucl. Phys.* **A661**, 23 (1999)
[8] CERES Collaboration: G Agakichiev *et al*, *Nucl. Phys.* in press
[9] HELIOS-1 Collaboration: T Akesson *et al*, *Z. Phys.* **C68**, 47 (1995)
[10] HELIOS-3 Collaboration: M Masera, *Nucl. Phys.* **A590**, 93c (1995)
HELIOS-3 Collaboration: A L S Angelis *et al*, CERN-EP/98-82
[11] NA38 Collaboration: A De Falco, *Nucl. Phys.* **A638**, 487c (1998)
[12] NA50 Collaboration: E Scomparin *et al*, *J. Phys.* **G25**, 235 (1999)
NA50 Collaboration: P Bordalo, *Nucl. Phys.* **A661**, 638 (1999)
[13] CERES Collaboration: R Baur *et al*, *Z. Phys.* **C71**, 571 (1996)
[14] HELIOS-2 Collaboration: T Akesson *et al*, *Z. Phys.* **C46**, 369 (1990)
[15] WA80 collaboration: R Albrecht *et al*, *Z. Phys.* **C51**, 1 (1991)

[16] WA80 Collaboration: R Albrecht *et al*, *Phys. Rev. Lett.* **76**, 3506 (1996)
[17] WA/98 Collaboration: M M Aggarwal *et al*, *Phys. Rev. Lett.* **85**, 3595 (2000)
[18] P Braun-Munzinger, I Heppe and J Stachel, *Phys. Lett.* **B465**, 15 (1999)
[18b] The standard pp cocktail, previously used in the presentation of the CERES results [2] and based on yields directly measured in pp collisions, predicts very similar results. The total yield of the present generator is $\sim$30 % larger than the pp cocktail for masses $m > 200$ MeV/c^2, the main difference occurring in the region of the ϕ meson.
[19] NA60 Proposal to CERN/SPSC 2000-010, SPSC/P 316, March 2000
[20] R Rapp and J Wambach, Preprint hep-ph/9909229 *Adv. Nucl. Phys.* (to appear)
[21] G Q Li, C M Ko and G E Brown, *Phys. Rev. Lett.* **75**, 4007 (1995)
[22] G E Brown and M Rho, *Phys. Rev. Lett.* **66**, 2720 (1991); *Phys. Rep.* **269**, 333 (1996)
[23] R Rapp, *Nucl. Phys.* **A661**, 33 (1999)
[24] R Rapp, G Chanfray and J Wambach, *Nucl. Phys.* **A617**, 472 (1997)
J Wambach, *Nucl. Phys.* **A638**, 171c (1998)
[25] J V Steele, H Yamagishi and I Zahed, *Phys. Rev.* **D56**, 5605 (1997)
J V Steele and I Zahed, *Phys. Rev.* **D60**, 037502 (1999)
[26] V Koch, nucl-th/9903008
V Koch and C Song, *Phys. Rev.* **C54**, 1903 (1996)
[27] E L Bratkovskaya and W Cassing, *Nucl. Phys.* **A619**, 413 (1997)
[28] W Cassing, E L Bratkovskaya, R Rapp and J Wambach, *Phys. Rev.* **C57**, 916 (1998)
[29] P Huovinen and M Prakash, *Phys. Lett.* **B450**, 15 (1999)
[30] R A Schneider and W Weise, *Europhys. J.* **A9**, 357 (2000)
[31] See e.g. D K Srivastava, B Sinha and C Gale, *Phys. Rev.* **C53**, R567 (1996)
R Rapp and J Wambach, *Europhys. J.* **A6**, 415 (1999)
[32] A Shor, *Phys. Lett.* **B215**, 375 (1988)
[33] G Q Li and C Gale, *Phys. Rev. Lett.* **81**, 1572 (1998)
[34] R Rapp and E Shuryak, *Phys. Lett.* **B473**, 13 (2000)
[35] K Gallmeister, B Kampfer and O P Pavlenko, *Phys. Lett.* **B473**, 20 (2000)
[36] G Q Li and G E Brown, *Nucl. Phys.* **A632**, 153 (1998)
[37] I Tserruya, *Nucl. Phys.* **A590**, 127c (1995)
[38] D K Srivastava, Preprint nucl-th/0102005
D K Srivastava and B Sinha, Preprint nucl-th/0006018
[39] F D Steffen and M H Thoma, Preprint hep-ph/0103044
[40] *Proc. of Quark Matter 2001*, to be published in *Nucl. Phys.*
[41] K Adcox *et al*, the PHENIX Collaboration: *Phys. Rev. Lett.* **86**, 3500 (2001)
[42] K Adcox *et al*, the PHENIX Collaboration: Preprint nucl-ex/0104015
[43] T Alber *et al*, NA49 Collaboration: *Phys. Rev. Lett.* **75**, 3814 (1995)
[44] B B Back *et al*, the PHOBOS Collaboration: hep-ex/0104032
[45] F Sickler *et al*, NA49 Collaboration: *Nucl. Phys.* **A661**, 45cc (1999)
[46] J D Bjorken, *Phys. Rev.* **D27**, 140 (1983)
[47] K Kajantie, J Kapusta, L McLerran and A Mekjian, *Phys. Rev.* **D34**, 2746 (1986)
[48] P V Ruuskanen, *Nucl. Phys.* **A544**, 169c (1992)
[49] C Adler *et al*, the STAR Collaboration: nucl-ex/0104022